Backstepping Mechanism of Kinesin-1

Algirdas Toleikis,[1] Nicholas J. Carter,[1] and Robert A. Cross[1,*]
[1]Centre for Mechanochemical Cell Biology, Warwick Medical School, Coventry, United Kingdom

ABSTRACT   Kinesin-1 is an ATP-driven molecular motor that transports cellular cargo along microtubules. At low loads, kinesin-1 almost always steps forward, toward microtubule plus ends, but at higher loads, it can also step backward. Backsteps are usually 8 nm but can be larger. These larger backward events of 16 nm, 24 nm, or more are thought to be slips rather than steps because they are too fast to consist of multiple, tightly coupled 8-nm steps. Here, we propose that not only these larger backsteps, but all kinesin-1 backsteps, are slips. We show first that kinesin waits before forward steps for less time than before backsteps and detachments; second, we show that kinesin waits for the same amount of time before backsteps and detachments; and third, we show that by varying the microtubule type, we can change the ratio of backsteps to detachments without affecting forward stepping. Our findings indicate that backsteps and detachments originate from the same state and that this state arises later in the mechanochemical cycle than the state that gives rise to forward steps. To explain our data, we propose that, in each cycle of ATP turnover, forward kinesin steps can only occur before Pi release, whereas backslips and detachments can only occur after Pi release. In the scheme we propose, Pi release gates access to a weak binding K·ADP-K·ADP state that can slip back along the microtubule, re-engage, release ADP, and try again to take an ATP-driven forward step. We predict that this rescued detachment pathway is key to maintaining kinesin processivity under load.

SIGNIFICANCE   Kinesin-1 molecular motors are ATP-driven walking machines that typically step forward toward microtubule plus ends. But they can also step backward, especially at high load. Backsteps are currently thought to occur by directional reversal of forward walking. On the contrary, we propose here that kinesin backsteps are not steps but slips. We show that backward translocations originate from a different and later state in the kinesin mechanism than the state that generates forward steps. To explain this, we propose that after ATP binding, kinesin molecules that fail to step forward within a load-dependent time window convert to a state that can slip back, rebind to the microtubule, and try again to step forward.

INTRODUCTION

Kinesin-1 is a ubiquitous, ATP-driven molecular motor that moves in 8-nm steps (1) toward the plus ends of cellular microtubules (MTs). To function effectively as an intracellular transporter (2,3), kinesin needs to move vesicles and other cargo up to several microns in diameter against appreciable hindering loads created by the crowded and dynamic intracellular environment. Understanding how kinesin makes sustained progress under load is an important problem. There is firm evidence that between steps, kinesin waits for ATP with one motor domain (the holdfast head) bound to the MT and the other (the tethered head) poised to step but pre-

vented from doing so until ATP binds (4–10). At low hindering loads, forward steps toward MT plus ends predominate, whereas at higher loads forward stepping slows down, and more backsteps are seen. It is clear that both forward steps (11–13) and backsteps (14,15) require ATP and that at stall, forward steps and backsteps are equally likely (14,15). Indeed, this property defines the stall force. Current models, including our own, envisage that backsteps occur by a hand-over-hand mechanism that resembles that for forward stepping but with load-dependent reversal of the directional bias (14–19). Nonetheless, it remains possible that forward and backward kinesin steps occur by different mechanisms.

MATERIALS AND METHODS

Kinesin beads

Unmodified 560-nm-diameter polystyrene beads (Polysciences, Warrington, PA) were mixed with purified recombinant full-length *Drosophila*
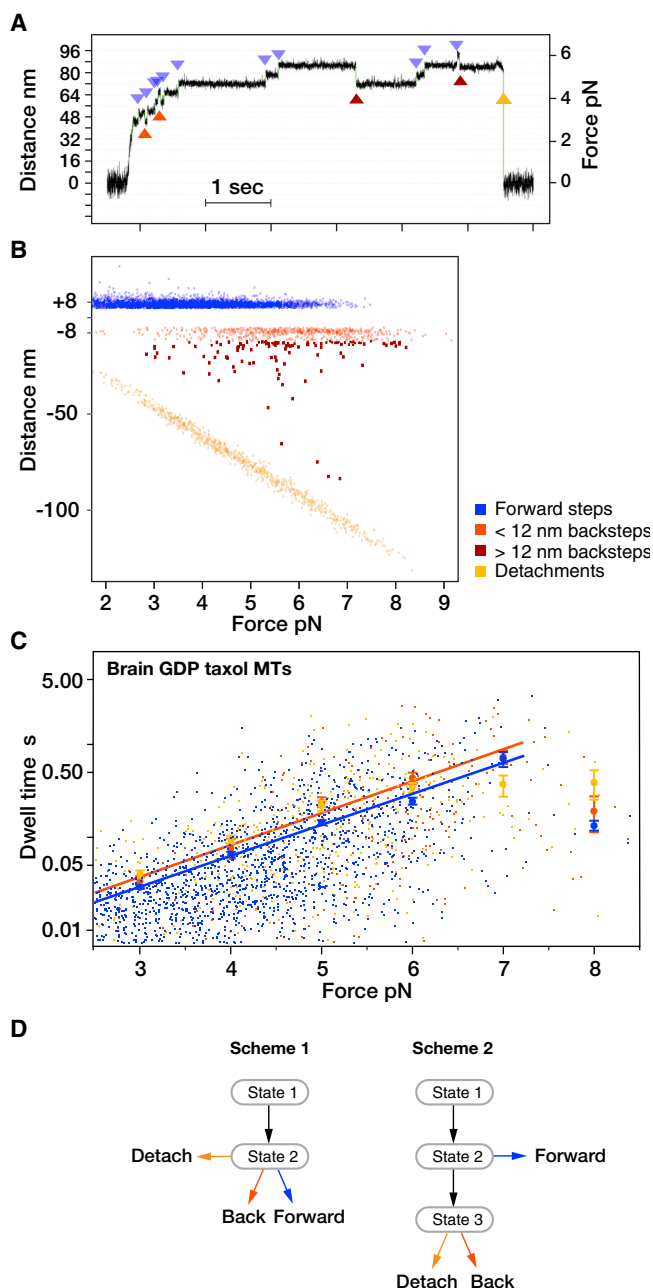

FIGURE 1 Stepping of single kinesin molecules on brain GDP Taxol MTs under load. (*A*) Representative sequence of kinesin steps, with examples of each step-class highlighted. (*B*) Step amplitudes and incidence versus hindering force for forward steps, backsteps, larger backsteps, and detachments. Trap stiffness for these experiments was ~0.06 pN/nm. (*C*) Forward step (*blue*), backstep (*red*), and detachment (*yellow*) dwell times versus hindering force for brain GDP MTs stabilized with Taxol. The larger symbols are mean dwell times calculated for bins set at 1-pN intervals. Below stall, dwell times depend exponentially on load; forward step dwell times are characteristically shorter than backstep or detachment dwell times, and backstep and detachment dwell times are indistinguishable. Approaching stall force on all types of MT, dwell times reach a plateau, above which further increases in force have little influence on dwell time [15]. Mean dwells up to the stall force (7.2 pN) were fitted by least squares using $\log(y) = kx + b$. Parameters are as follows: blue, $k = 0.77$, $b = -5.7$; or-

kinesin-1 [12], serially diluted until only one-third of beads were motile. Experiments were performed in BRB80 buffer (80 mM K-PIPES (pH 7.0), 2 mM $MgSO_4$, 1 mM EGTA, 3 g/L glucose) with 1 mM ATP and glucose-catalase oxygen scavenging system and 10 μM Taxol or 10 μM epothilone or with no drug.

MTs

Purified tubulin (either from porcine brain or from *Schizosaccharomyces pombe* (*α1*, *α2*, *β* isoforms [20])) was polymerized in BRB80 at 37°C for 45–60 min in the presence of 1 mM GTP and 2 mM $MgCl_2$. MTs were spun down and resuspended in BRB80 supplemented with Taxol (Sigma-Aldrich, St. Louis, MO) or epothilone (VWR International, Radnor, PA) to 20 μM. Because Taxol is not effective on *S. pombe* MTs, epothilone was used instead, in combination with guanosine-5'-[(α,β)-methyleno] triphosphate (GMPCPP). In the case of unstabilized guanosine-5'-diphosphates (GDP MTs), no drug was added, but MTs were capped immediately after assembly using tubulin premixed with 1 mM GMPCPP and incubated for 1 h, added to a final concentration of 1 μM. The capped MTs were spun down and resuspended in BRB80.

Flow cells

The flow cell surface was passivated with 0.1 mg/mL poly(L-Lysine)-*g*-Poly(Ethylene Glycol) (PLL-PEG) and then with 0.1 mg/mL casein (SuSoS AG, Dübendorf, Switzerland). MTs were covalently attached to the coverslip surface using mild glutaraldehyde cross-linking to the 3-Aminopropyl)triethoxysilane (APTES)-silanized surface [21].

Optical trapping

A custom-built optical trap [15] was used, equipped with a 3-W Nd:YAG 1064-nm laser (IE Optomech, Newnham, England). High-ionic-strength experiments were performed in BRB160, which is identical to BRB80 but with 160 mM K-PIPES. MTs were initially visualized by differential interference contrast microscopy, and beads were moved into position above the MTs by steering the trap. Imaging was then switched to amplitude contrast, and the image was projected onto the quadrant photodiode detector. Data were recorded at 20 kHz, and the moving average was filtered to 1 kHz during analysis.

Data analysis

Data were analyzed in R using custom-written code (available on request). Automated step-detection was implemented using *t*-test analysis. In the *t*-test analysis, eight data points before the suspected step and eight after the step were compared by *t*-test. The threshold *t*-value was set to 30, and the minimal step size was set to 5 nm. Dwell times were defined as the waiting time between two consecutive steps. ~30–40% of the longest dwells in each force bin were manually verified to ensure that there were no undetected steps within these dwells. Only steps above 2 pN could reliably be detected, and only these were processed. Below 3-pN backsteps were rare, and above 8-pN forward steps were rare. For forward step/backstep ratio measurements, the force range 3–8 pN was analyzed to ensure a sufficient number of both forward steps and backsteps. Each force bin includes data at the force shown ± 0.5 pN.

ange, $k = 0.79$, $b = -5.6$. Errors are mean ± standard error (SE). (*D*) Minimal schemes for the kinesin mechanism (see text) are given. To see this figure in color, go online.

RESULTS AND DISCUSSION

Dwell times for forward steps are shorter than dwell times for backsteps

To test this point experimentally, we compared the average dwell times for forward steps, backsteps, and detachments for kinesin moving on various types of MT. The dwell times are the waiting times preceding each step, consisting of the time spent waiting for ATP to bind plus the time taken to process ATP and complete the coupled mechanical step. We also made counts of forward steps, backsteps (on average 8 nm, but up to 12 nm), larger backsteps (>12 nm), and full detachments for kinesin stepping under defined hindering loads between 2 and 9 pN applied with an optical trap (Fig. 1, A and B). In a full detachment, the motor releases completely from the MT, causing the bead-motor complex to relax back into the center of the optical trap (Fig. 1 A).

For kinesin-1 moving on Taxol-stabilized pig brain GDP MTs, the general form of the dwell time versus load relationship is as previously reported (14–17); forward-step dwell times are exponentially dependent on load at forces up to and including the stall force (Fig. 1 C). Crucially, however, we find that at any particular substall load, forward steps have shorter average dwell times than either backsteps or detachments (Fig. 1 C), whereas backsteps and detachments have similar or identical average dwell times (see next section). Previous work, including our own, has assigned backsteps and forward steps as alternative outcomes from the same state in the kinesin mechanism (14,15). Correspondingly, current kinesin schemes postulate a minimum of two bound mechanical states (Fig. 1 D, scheme 1). In scheme 1, ATP binds to state 1, the waiting state, and converts it to state 2, the stepping state, which then either steps forward or backward or detaches, depending on load. Because in scheme 1, forward and backward steps originate from the same state, their dwell times are drawn from the same distribution. However, we now find that average dwell times for forward steps are shorter than those for backsteps and detachments, whereas those for backsteps and detachments are indistinguishable. To explain this, we need a scheme with a minimum of three states, with ATP binding creating state 2, the try-forward state, and Pi release creating state 3, the backsteps-and-detachments state (Fig. 1 D, scheme 2). A three-state scheme is the minimal scheme required to produce different dwell-time distributions for forward and backward steps.

The difference between mean forward and backstep dwell times for kinesin moving on GDP Taxol brain MTs is just a few milliseconds at a 3-pN load, increasing approximately exponentially to several tens of milliseconds at a 6-pN load (Fig. 1 C). On other types of MT lattice, average forward and backstep dwell times are more obviously different.

We measured kinesin-1 single-molecule stepping mechanics on brain GDP Taxol MTs, brain GDP MTs without Taxol, brain GMPCPP epothilone MTs, and *S. pombe* GMPCPP epothilone MTs. Epothilone is an MT-binding drug that stabilizes both brain and yeast MTs, whereas Taxol only stabilizes brain MTs. Previous work has shown that the nucleotide state of tubulin can influence MT sliding velocity in unloaded motility assays (22). Lattice expansion and other lattice effects due to changes in nucleotide state (23), drug occupancy (24), or kinesin occupancy (25,26) can also potentially influence kinesin binding and stepping at low load. Under load in an optical trap, we find that changing MT lattice type, indeed, substantially affects kinesin stepping mechanics. Most obviously, stalls are shorter on brain MTs (Fig. 2 A) than on *S. pombe* MTs (Fig. 2 C), indicating that detachment of kinesin-1 while stepping at high load is more probable for brain MTs.

Dwell times for backsteps and detachments are the same

For all the types of MT that we tried, we find not only that mean forward-step dwell times at substall forces are shorter than those for backsteps and detachments but also that mean dwell times for 8-nm backsteps, longer backsteps, and detachments appear identical (Figs. 1 C and 2, B and D), reflecting that the dwell-time distributions for 8-nm backsteps, longer backsteps, and detachments superpose and implying that these different types of events originate from the same state in the kinesin mechanism (16,17). Because backstep and detachment dwell times are longer on average than forward-step dwell times, their progenitor state must occur later in each cycle of the mechanism than the state that generates forward steps (Fig. 1 D, scheme 2).

Counts of backsteps and detachments vary reciprocally on different MT lattices

Making counts of forward steps, backsteps, and detachments at each load gives further insight. The balance between 8-nm backsteps, longer backsteps, and detachments at any particular load shifts substantially depending on the type of MT lattice, whereas the fraction of forward steps is little affected (Fig. 3, A–D). The ratio #forward steps/#backsteps decreases exponentially with load, as previously reported (14,15), but both the exponential factor and the stall force are different for the different MT lattices (Fig. 3 E). Stall force is defined as the force at which #forward steps equals #backsteps. For GDP Taxol brain MTs, stall force is 7.3 ± 0.2 pN, as previously reported (14,15), whereas for the other types of MT, stall force is 6.4 ± 0.1 pN (Fig. 3 E, *p*-value < 0.001 vs. GDP Taxol brain MTs). By contrast, the ratio #forward steps/{#backsteps + #detachments} versus load is almost invariant for the different types of MT (Fig. 3 F), reflecting
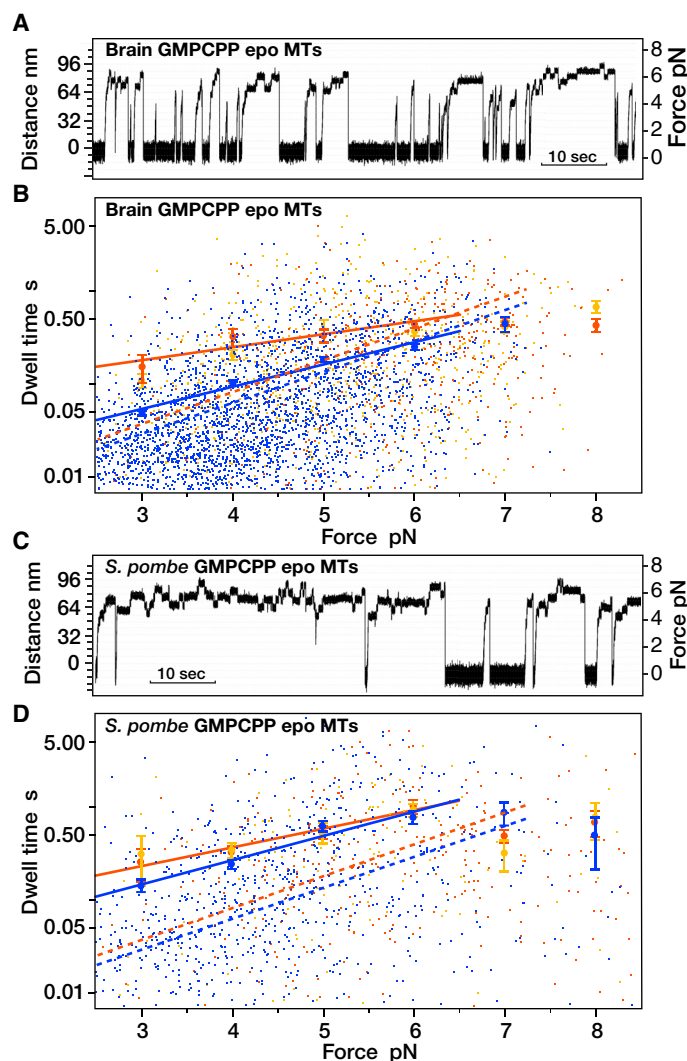
FIGURE 2 Mechanics of kinesin stepping under load on different MT types. (*A* and *C*) Optical trapping position versus time traces show the much shorter stalls typically seen with brain GMPCPP epothilone MTs (*A*) compared with *S. pombe* GMPCPP epothilone MTs (*C*). (*B* and *D*) Dwell times versus load for kinesin stepping on (*B*) brain GMPCPP epothilone MTs and (*D*) *S. pombe* GMPCPP epothilone MTs. As in Fig. 1 *C*, dwell times depend exponentially on load, mean forward-step dwell times are characteristically shorter than mean backstep or detachment dwell times, and mean backstep and detachment dwell times are indistinguishable. Approaching stall force, backstep dwell times reach a plateau, above which further increases in hindering load have little effect on dwell time (15). Mean dwell times in the region below stall force were fitted using $log(y) = kx + b$. Parameters are as follows: (*B*) blue, k = 0.53, b = −4.4; orange, k = 0.25, b = −2.3; (*D*) blue, k = 0.6, b = −3.6; orange, k = 0.46, b = −2.7. Errors are mean ± SE. In (*B*) and (*D*), fits for GDP Taxol MTs are shown for comparison (*dotted lines*). To see this figure in color, go online.

that switching MT lattice type changes the relative incidence of 8-nm backsteps, longer backsteps, and detachments, without appreciably changing the count of forward steps or the total count of #backsteps + #detachments at any particular load (Fig. S1). This is only possible in a three-state minimal scheme (Fig. 1 *D*), in which backsteps and detachments are alternative outcomes from state 3 and forward steps originate from a different and earlier state, state 2. Because detachments and backsteps both originate from state 3, we hypothesized that state 3 is a weak binding state that can diffuse back along the MT and then convert to strong binding to complete a backstep. To test this idea, we varied conditions further.

Added ADP inhibits forward steps and promotes backsteps and detachments

K·ADP is the weakest state of the kinesin cycle (27,28). If, as we hypothesize, state 3 is a K·ADP state, then adding ex-

tra ADP to the bathing solution should enrich state 3 via ADP binding to the waiting state. To test this possibility, we recorded kinesin stepping under load on brain GDP Taxol MTs, in the presence of added ADP (Fig. 4 *B*). Increasing [ADP] without changing [ATP] favors backstepping and disfavors forward stepping (Fig. 4 *B*), thereby reducing stall force from 7.3 ± 0.2 to 5.1 ± 0.2 pN (Fig. 4 *E*). More detailed counts show that added ADP not only produces more backsteps but also adds a population of longer backsteps (Fig. S2). These data indicate that adding ADP enriches state 3, from which backsteps and detachments arise (Fig. 1 *D*), consistent with state 3 being a K·ADP-K·ADP state and with added ADP enriching the K·ADP-K·ADP state by binding to the waiting state (the K–K·ADP state). Dwell-time distributions (Fig. 5) show that added ADP increases the average forward-step dwell time at low load and abrogates forward stepping at high load, consistent with the main element of dwell time under load being the waiting time before nucleotide binding and
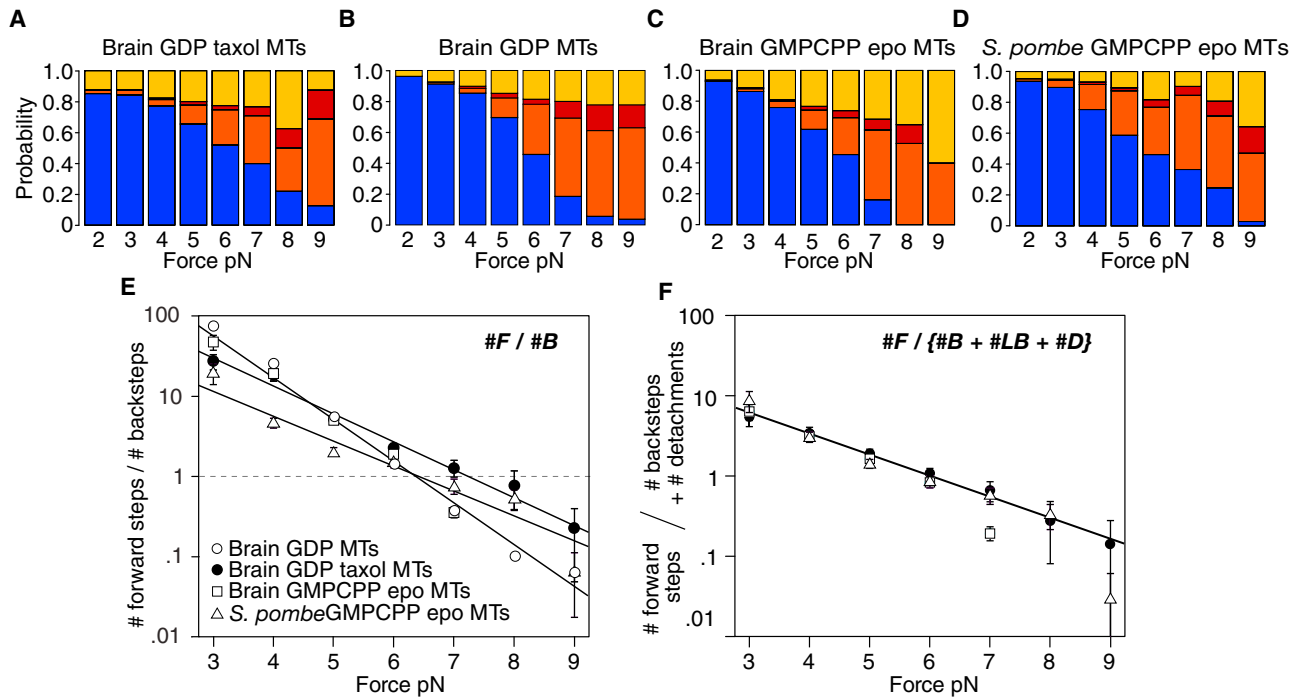
FIGURE 3 Effects of changing MT type on step-event probabilities under load. (*A–D*) Probability of forward steps (*blue*), <12-nm backsteps (*orange*), >12-nm backsteps (*magenta*), and detachments (*yellow*) versus force for kinesin stepping on (*A*) brain GDP Taxol MTs, (*B*) brain GDP MTs, (*C*) brain GMPCPP epothilone MTs, and (*D*) *S. pombe* GMPCPP epothilone MTs. (*E*) #forward steps/#backsteps versus force for kinesin stepping on these four different MT types. Data were fitted to $\log(y) = kx + b$, weighting the fit by the reciprocal SE. For brain GMPCPP epothilone MTs, $k = -1.16$, $b = 7.45$; for *S. pombe* GMPCPP epothilone MTs, $k = -0.79$, $b = 5.0$; for brain GDP Taxol MTs, $k = -0.83$, $b = 5.9$. Errors are SE. (*F*) #forward steps/ {#backsteps + #larger backsteps + #detachments} versus force, for kinesin stepping on different MT types is shown. Fit shown is to brain GDP Taxol MTs data, $k = -0.58$, $b = 3.5$. To see this figure in color, go online.

with added ADP competing directly with ATP for binding to the waiting state. The change in the dwell time distribution caused by adding ADP (Fig. 5) suggests that some events might involve multiple rounds of ADP release and rebinding.

Increased ionic strength promotes detachment

By increasing ionic strength, we expect to weaken our hypothesized weak binding K·ADP-K·ADP state 3 because weak binding has a considerable electrostatic component (29). We find that, indeed, increased ionic strength promotes detachment, with much smaller effects on ~8-nm backsteps and longer backsteps (Fig. 4 *C*), consistent with increased ionic strength weakening and depopulating the K·ADP-K·ADP state without appreciably affecting forward stepping. As a result, stall force is only marginally reduced (Fig. 4 *E*).

Subtilisin treatment of MTs lengthens backsteps and inhibits detachment

Cleaving the C-terminal E-hook peptides of tubulin (30) has only slight effects on kinesin velocity at low load but reduces processivity (31). To further probe the nature of our

envisaged semidetached state, we cleaved the E-hooks from GDP Taxol MTs using subtilisin and again examined stepping mechanics under load. Subtilisin digestion has little or no effect on the tendency to take forward steps relative to all other events (Fig. 4 *D*). Subtilisin digestion does, however, increase the probability of long (>12 nm) backsteps and decrease the probability of detachments. These data again demonstrate that the balance between short backsteps, long backsteps, and detachments can be shifted substantially by experiment without affecting forward stepping, consistent with our contention that forward steps originate from a different and earlier state in the kinesin mechanism than the state generating backsteps and detachments.

Proposed model

Our key finding is that dwell times for kinesin backsteps, long backsteps, and detachments are drawn from the same dwell-time distribution, whereas the dwell times for forward steps are drawn from a different distribution with a shorter mean dwell time. Scheme 2 (Fig. 1 *D*) is the minimal scheme necessary to explain how shifting kinesin between different MT types can shift the balance between backsteps and detachments without affecting forward stepping. Scheme 1, in which forward steps and backsteps originate
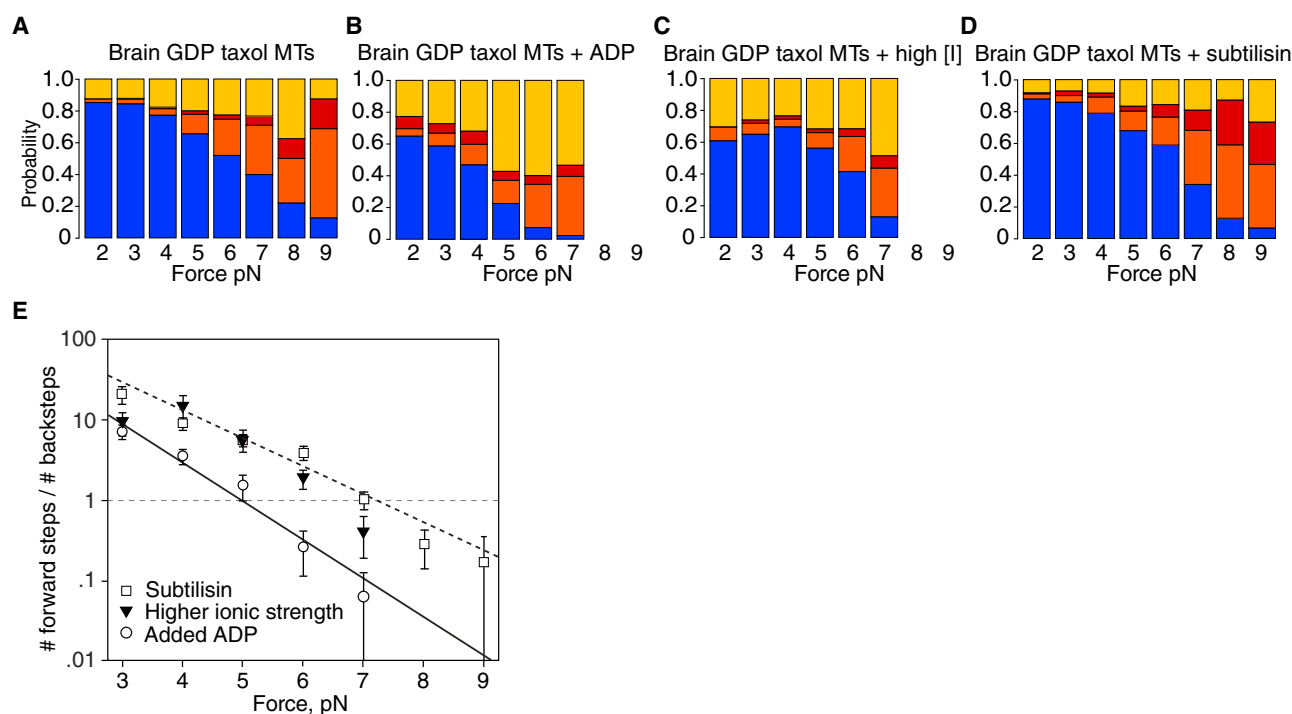
FIGURE 4 Effects of changing conditions on step-event probabilities under load. (*A*) Brain GDP Taxol MTs, as in Fig. 3 *A*. (*B*) Brain GDP Taxol MTs with added 1 mM ADP. (*C*) Brain GDP Taxol MTs at higher ionic strength (BRB160 instead of BRB80). (*D*) Brain GDP Taxol MTs treated with subtilisin. (*E*) Effects of ADP, higher ionic strength and subtilisin treatment on #forward steps/#backsteps ratio for kinesin stepping on GDP-Taxol MTs under hindering load. ADP data fit parameters are as follows: k = −0.69, b = 4.9. Broken black line is the fit for stepping on GDP Taxol MTs from Fig. 3 *E*. Errors are SE. To see this figure in color, go online.

from the same state, is ruled out because in scheme 1, forward steps and backsteps originate from the same state and so should share the same dwell-time distribution, and we have shown that they do not.

How might scheme 2 map to the kinetic mechanism of kinesin? In our proposed new, to our knowledge, model (Fig. 6), ATP binding opens a time window devoted exclusively to forward stepping. Within this time window, our scheme allows for forward stepping under load from either the ATP or the ADP·Pi states of the holdfast head (Fig. 6, *blue pathway*). We include both these possibilities because, although recent evidence points to the K·ADP·Pi-K·ADP

state as the origin of forward steps at zero load (10), the effects of load on the hydrolysis step are not yet clear. It is possible, for example, that the hydrolysis step might be reversible under load, as it is for myosin (32,33). In our model, the forward-step time window is closed by Pi release (34), and we propose that backsteps and detachments occur only after Pi release. We envisage that, at high hindering loads, forward stepping increasingly fails to occur within its time window and that closure of this time window by Pi release switches the motor into a weakly bound K·ADP-K·ADP state (Fig. 6, *orange pathway*). In our scheme, this K·ADP-K·ADP state then typically slips

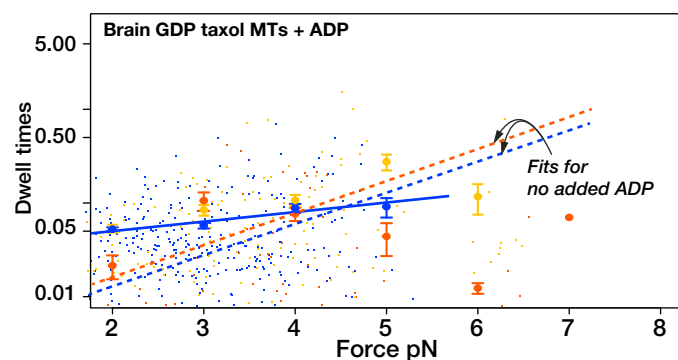
FIGURE 5 Dwell-time distributions with added ADP. "Fits for stepping on GDP Taxol MTs without added ADP (Fig 1B) are shown as dotted lines, for reference. Adding ADP reduces the load dependence of the mean dwell time for forward steps. Errors are SE. To see this figure in color, go online.
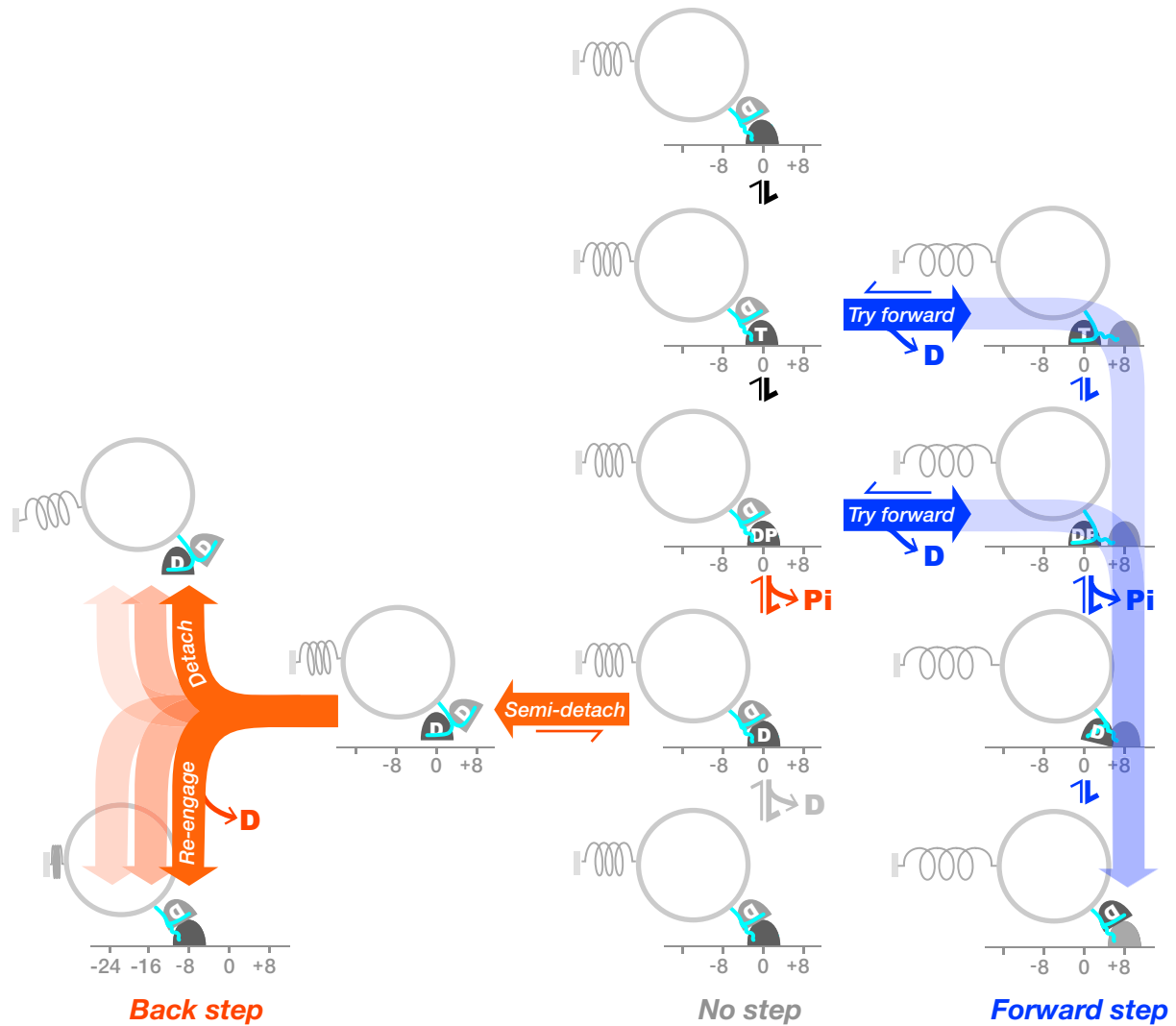
FIGURE 6 Proposed new, to our knowledge, model for kinesin stepping under load. The key feature of the model is that forward steps and backward steps originate from different states. During each cycle of ATP turnover under load, kinesin first attempts to step forward from its K·ATP-K·ADP and K·ADP·Pi-K·ADP states (*blue arrows*). In our model, backsteps do not occur from either of these states. At higher loads, forward stepping increasingly fails to complete before Pi release, and kinesin then enters a weak binding K·ADP-K·ADP state that can slip back along the lattice (*orange arrows*), re-engage, release ADP, and begin a fresh attempt to step forward. For completeness, a presumptively minor process, ADP release while standing still (*gray arrows*), is also shown. To see this figure in color, go online.

back along the lattice, re-engages, releases ADP, and returns to its K–K·ADP waiting state, completing a de facto backstep. Under backward load, re-engagement typically occurs to the closest available tubulin heterodimer, resulting in an 8-nm backslip. Less routinely, backslips of 16 or 24 nm can occur, or the motor can fully detach. For completeness, we include a presumptively off-pathway transition, in which MT-activated ADP release occurs with the motor standing in place (Fig. 6, *gray arrows*). It is unclear at present to what extent this pathway, which would produce futile cycles at high load, is used. It is also unclear whether our K·ADP-K·ADP slip state rebinds to the same protofilament (PF) from which it unbound or to a different PF. We also do not yet know whether after a slip, the same head that de-

tached then re-engages or whether the two heads can swap over. Distributions of backstep sizes may provide a clue. Counts of backsteps in each size class reveal approximately exponentially decreasing likelihoods of 8, 16, 24, and 32 nm backsteps under load for each of the MT lattice types that we tested (Fig. 7, *A–D*). This suggests a fixed probability of rebinding (rescue) of our hypothesized K·ADP-K·ADP slip state at each subunit position back along a single PF, but further work will be needed to clarify this point.

Relationship to other models

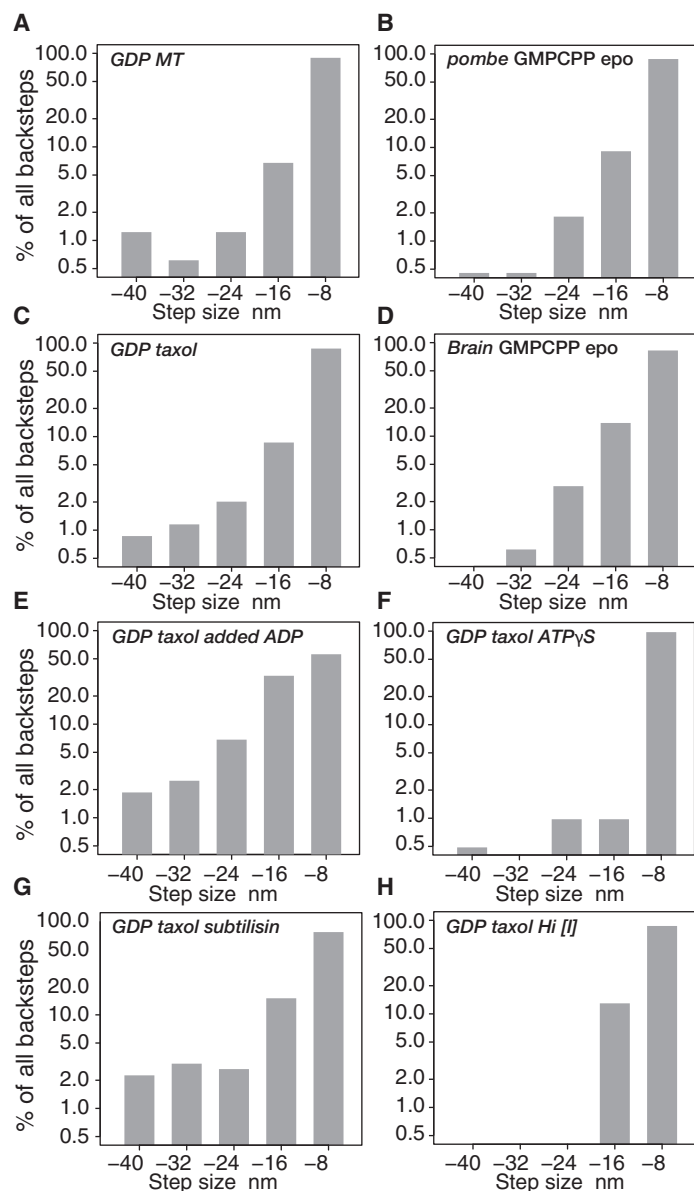Our new model (Fig. 6) is conventional in that ATP binding directly or indirectly gates forward stepping, with gating

FIGURE 7   Backstep size distributions. (*A–H*) Percentage of all backward events in each size class for different MT lattices and in different conditions is shown. Note that *y* axis is on a log scale. (*A–D*) Different MT lattices are shown. Probability distributions appear roughly exponential, consistent with backsteps being backslips that have an equal probability of reattachment at each position back along a single PF toward the MT-minus end. (*E* and *F*) Under perturbation, this exponential relationship no longer holds. In (*E*) and (*G*), longer backsteps appear more probable. In (*F*) and (*H*), longer events are very rare.

involving a combination of ATP-dependent unparking of the leading (tethered) head (4,5,35,36) and ATP-dependent stabilization of neck linker docking on the MT-attached trail head (37–40). Assigning K·ADP as the weakest binding state in the cycle is also conventional (27,28), and our assignment of the K·ADP-K·ADP state as the detaching state is also consistent with earlier models (10,15,41). The idea that some backward events are slips is also not novel; 16-, 24-nm, and larger backward displacements have previously been assigned as slips on the basis that they are too fast to represent a sequence of 8-nm steps that are each coupled to a full cycle of ATP turnover (15). The novel aspects of our proposed scheme are first that the interlude between ATP binding and Pi release (the hydrolysis time) is devoted exclusively to forward stepping; second, that all backward events at substall loads are backslips; and third, that backslips and detachments arise from the same K·ADP-K·ADP state.

Our proposed scheme is consistent with recent work showing that the rate of kinesin stepping can be influenced either by supplying extra ADP to inhibit tethered head attachment or by lowering ionic strength to strengthen the binding of the K·ADP state to the MT (10). At zero external load, backsteps are rarely seen, but our data suggest that similar effects may operate, that is, that increased [ADP] and ionic strength, respectively, enrich or deplete a weakbound K·ADP-K·ADP slip state (42).

Slip and re-engage behavior under backward load has been seen before in kinesins. We previously assigned 16-nm and larger backward kinesin-1 events as slips (15).

Jannasch et al. (43) showed that backslipping of Kip3, the *Saccharomyces cerevisiae* kinesin-8, limits its stall force to <1 pN. The claim we make here is that 8-nm kinesin-1 backsteps are also slips, so that a slip-and-re-engage pathway is integral to the mechanism of a transport kinesin that can do appreciable mechanical work.

Our proposed scheme is also consistent with recent work showing that adding Pi extends the single-molecule run length of kinesin-1 (34) under forward load because it predicts that adding Pi will enrich the K·ADP·Pi-K·ADP state and so delay the formation of the backslipping K·ADP-K·ADP state. Equally, our scheme is consistent with models in which slower ATP hydrolysis promotes forward stepping by promoting diffusion to capture by the tethered head (10,44) because slower ATP hydrolysis would allow more time for forward stepping. We attempted to test this last point directly, using adenosine-5'-(3-thio)-triphosphate ATPγS), an ATP analog that drives MT sliding assays at ~2–3% of ATP velocity (45). Using interferometric scattering microscopy (iSCAT), ATPγS was recently shown to support slow, erratic stepping of single kinesin-1 molecules at zero load (46). Under load in the optical trap, we find that ATPγS also drives slow and erratic stepping of kinesin-1 (Fig. 8 A). However, we find that the MT-activated rate of ATPγS turnover by kinesin in solution is only six- to sevenfold lower than that for ATP (Fig. 8 D). These data suggest that ATPγS is hydrolyzed relatively rapidly but has poor mechanochemical coupling, so that at present, it does not provide a useful test of our scheme.

Implications

Most immediately, our proposed new, to our knowledge, model (Fig. 6) has implications for the mechanochemical coupling of kinesin. As with previous models, in our new, to our knowledge, model, kinesin consumes more ATP at high loads because backslips consume ATP. In our scheme, even a single 8-nm backslip will consume one ATP to slip back 8 nm and another to step forward to regain its original position. Longer backslips will require correspondingly more ATP-driven forward steps to regain the ground lost. In one sense, these backslips are futile because they require ATP turnover and generate negative progress. In another sense, however, they are far from futile because they create the opportunity to retry forward stepping under load without
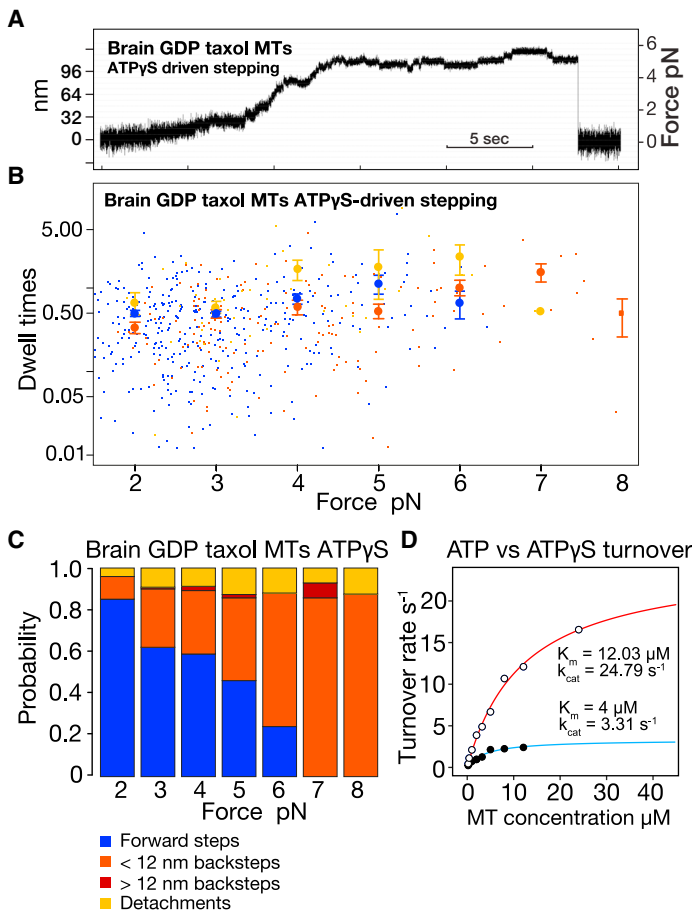

FIGURE 8 ATPγS-driven stepping. (*A*) Representative optical trapping record. Stepping is slow, and steps are less well defined than in ATP, especially at low loads. (*B*) Dwell time versus load plot for forward steps, backsteps, and detachments. Errors are SE. Dwell times appear less load-dependent than in ATP. (*C*) Event probabilities versus load. Errors are SE. Backsteps appear much more probable than in ATP (compare with Fig. 3 *A*). (*D*) Nucleotide turnover for ATP (*red fit*) versus ATPγS (*blue fit*). To see this figure in color, go online.

letting go of the MT and losing all the ground previously gained. A further possible pathway for futile cycling is denoted by the gray arrow in Fig. 6, corresponding to MT-activated ADP release without stepping. At present, we have no information on the flux through this pathway, which would also consume ATP but without losing ground.

Although our data argue that the large majority of kinesin-1 backward translocations are slips, we cannot exclude that a small fraction of true mechanical "hand-over-hand" backsteps, as opposed to backslips, is present. However, because these events would originate from the same state that generates forward steps, they would draw from the same dwell-time distribution as forward steps (Fig. 1 D, scheme 1) and tend to make the dwell-time distribution for 8-nm backsteps more like that for forward steps, whereas we see that the dwell-time distribution for 8-nm backsteps is different from that for forward steps and indistinguishable from that for long backsteps and detachments. On this basis, we can firmly conclude that at least the great majority of backsteps are slips.

By rescuing kinesins that have failed to step forward within a load-dependent time window and allowing them to retry forward stepping, our proposed rescued detachment pathway increases the ultimate success rate for processive forward stepping under load, with a corresponding increase in stall force and the ability to do useful mechanical work. These gains come at the expense of extra ATP consumption, so that the ATP cost of each net forward step increases substantially at high loads. Effectively, backstepping via rescued detachment allows kinesin-1 to change gear under load by adaptively combining tightly coupled forward steps with loosely coupled backslips.

SUPPORTING MATERIAL

Supporting Material can be found online at https://doi.org/10.1016/j.bpj.2020.09.034.

AUTHOR CONTRIBUTIONS

A.T. performed all the experiments and analyzed all the data. N.J.C. designed and built the optical trap. A.T., N.J.C., and R.A.C. collaborated to design and interpret experiments and write the manuscript.

ACKNOWLEDGMENTS

REFERENCES

1. Block, S. M., L. S. Goldstein, and B. J. Schnapp. 1990. Bead movement by single kinesin molecules studied with optical tweezers. *Nature.* 348:348–352.

2. Karsenti, E. 2008. Self-organization in cell biology: a brief history. *Nat. Rev. Mol. Cell Biol.* 9:255–262.

3. Hirokawa, N., and Y. Tanaka. 2015. Kinesin superfamily proteins (KIFs): various functions and their relevance for important phenomena in life and diseases. *Exp. Cell Res.* 334:16–25.

4. Hackney, D. D. 1994. Evidence for alternating head catalysis by kinesin during microtubule-stimulated ATP hydrolysis. *Proc. Natl. Acad. Sci. USA.* 91:6865–6869.

5. Alonso, M. C., D. R. Drummond, …, R. A. Cross. 2007. An ATP gate controls tubulin binding by the tethered head of kinesin-1. *Science.* 316:120–123.

6. Mori, T., R. D. Vale, and M. Tomishige. 2007. How kinesin waits between steps. *Nature.* 450:750–754.

7. Guydosh, N. R., and S. M. Block. 2009. Direct observation of the binding state of the kinesin head to the microtubule. *Nature.* 461:125–128.

8. Andreasson, J. O. L., B. Milic, …, S. M. Block. 2015. Examining kinesin processivity within a general gating framework. *eLife.* 4:e07403.

9. Isojima, H., R. Iino, …, M. Tomishige. 2016. Direct observation of intermediate states during the stepping motion of kinesin-1. *Nat. Chem. Biol.* 12:290–297.

10. Mickolajczyk, K. J., and W. O. Hancock. 2017. Kinesin processivity is determined by a kinetic race from a vulnerable one-head-bound state. *Biophys. J.* 112:2615–2623.

11. Hua, W., E. C. Young, …, J. Gelles. 1997. Coupling of kinesin steps to ATP hydrolysis. *Nature.* 388:390–393.

12. Coy, D. L., M. Wagenbach, and J. Howard. 1999. Kinesin takes one 8-nm step for each ATP that it hydrolyzes. *J. Biol. Chem.* 274:3667–3671.

13. Schnitzer, M. J., and S. M. Block. 1997. Kinesin hydrolyses one ATP per 8-nm step. *Nature.* 388:386–390.

14. Nishiyama, M., H. Higuchi, and T. Yanagida. 2002. Chemomechanical coupling of the forward and backward steps of single kinesin molecules. *Nat. Cell Biol.* 4:790–797.

15. Carter, N. J., and R. A. Cross. 2005. Mechanics of the kinesin step. *Nature.* 435:308–312.

16. Taniguchi, Y., M. Nishiyama, …, T. Yanagida. 2005. Entropy rectifies the Brownian steps of kinesin. *Nat. Chem. Biol.* 1:342–347.

17. Taniguchi, Y., P. Karagiannis, …, T. Yanagida. 2007. Single molecule thermodynamics in biological motors. *Biosystems.* 88:283–292.

18. Carter, N. J., and R. A. Cross. 2012. Kinesin backsteps. *Biochem. Soc. Trans.* 40:400–403.

19. Guydosh, N. R., and S. M. Block. 2006. Backsteps induced by nucleotide analogs suggest the front head of kinesin is gated by strain. *Proc. Natl. Acad. Sci. USA.* 103:8054–8059.

20. Drummond, D. R., S. Kain, …, R. A. Cross. 2011. Purification of tubulin from the fission yeast *Schizosaccharomyces pombe. Methods Mol. Biol.* 777:29–55.

21. Nicholas, M. P., L. Rao, and A. Gennerich. 2014. Covalent immobilization of microtubules on glass surfaces for molecular motor force measurements and other single-molecule assays. *Methods Mol. Biol.* 1136:137–169.

22. Vale, R. D., C. M. Coppin, …, R. A. Milligan. 1994. Tubulin GTP hydrolysis influences the structure, mechanical properties, and kinesin-driven transport of microtubules. *J. Biol. Chem.* 269:23769–23775.

23. Hyman, A. A., D. Chrétien, …, R. H. Wade. 1995. Structural changes accompanying GTP hydrolysis in microtubules: information from a slowly hydrolyzable analogue guanylyl-(alpha,beta)-methylene-diphosphonate. *J. Cell Biol.* 128:117–125.

24. Arnal, I., and R. H. Wade. 1995. How does taxol stabilize microtubules? *Curr. Biol.* 5:900–908.

25. Peet, D. R., N. J. Burroughs, and R. A. Cross. 2018. Kinesin expands and stabilizes the GDP-microtubule lattice. *Nat. Nanotechnol.* 13:386–391.

26. Shima, T., M. Morikawa, …, N. Hirokawa. 2018. Kinesin-binding-triggered conformation switching of microtubules contributes to polarized transport. *J. Cell Biol.* 217:4164–4183.

27. Romberg, L., and R. D. Vale. 1993. Chemomechanical cycle of kinesin differs from that of myosin. *Nature*. 361:168–170.

28. Crevel, I. M., A. Lockhart, and R. A. Cross. 1996. Weak and strong states of kinesin and ncd. *J. Mol. Biol.* 257:66–76.

29. Uemura, S., K. Kawaguchi, …, S. Ishiwata. 2002. Kinesin-microtubule binding depends on both nucleotide state and loading direction. *Proc. Natl. Acad. Sci. USA*. 99:5977–5981.

30. Okada, Y., and N. Hirokawa. 2000. Mechanism of the single-headed processivity: diffusional anchoring between the K-loop of kinesin and the C terminus of tubulin. *Proc. Natl. Acad. Sci. USA*. 97:640–645.

31. Lakämper, S., and E. Meyhöfer. 2005. The E-hook of tubulin interacts with kinesin's head to increase processivity and speed. *Biophys. J.* 89:3223–3234.

32. Bagshaw, C. R., D. R. Trentham, …, P. D. Boyer. 1975. Oxygen exchange in the gamma-phosphoryl group of protein-bound ATP during Mg2+-dependent adenosine triphosphatase activity of myosin. *Proc. Natl. Acad. Sci. USA*. 72:2592–2596.

33. Webb, M. R., and D. R. Trentham. 1981. The mechanism of ATP hydrolysis catalyzed by myosin and actomyosin, using rapid reaction techniques to study oxygen exchange. *J. Biol. Chem.* 256:10910–10916.

34. Milic, B., J. O. L. Andreasson, …, S. M. Block. 2014. Kinesin processivity is gated by phosphate release. *Proc. Natl. Acad. Sci. USA*. 111:14136–14140.

35. Hackney, D. D. 2002. Pathway of ADP-stimulated ADP release and dissociation of tethered kinesin from microtubules. Implications for the extent of processivity. *Biochemistry*. 41:4437–4446.

36. Cross, R. A., I. Crevel, …, L. A. Amos. 2000. The conformational cycle of kinesin. *Philos. Trans. R. Soc. Lond. B Biol. Sci.* 355:459–464.

37. Rice, S., A. W. Lin, …, R. D. Vale. 1999. A structural change in the kinesin motor protein that drives motility. *Nature*. 402:778–784.

38. Khalil, A. S., D. C. Appleyard, …, M. J. Lang. 2008. Kinesin's cover-neck bundle folds forward to generate force. *Proc. Natl. Acad. Sci. USA*. 105:19247–19252.

39. Hwang, W., M. J. Lang, and M. Karplus. 2010. Free energy changes during kinesin's force-generating substep. *Biophys. J.* 98:369a.

40. Budaitis, B. G., S. Jariwala, …, K. J. Verhey. 2019. Neck linker docking is critical for kinesin-1 force generation in cells but at a cost to motor speed and processivity. *eLife*. 8:e44146.

41. Sasaki, K., M. Kaya, and H. Higuchi. 2018. A unified walking model for dimeric motor proteins. *Biophys. J.* 115:1981–1992.

42. Cross, R. A. 2004. The kinetic mechanism of kinesin. *Trends Biochem. Sci.* 29:301–309.

43. Jannasch, A., V. Bormuth, …, E. Schäffer. 2013. Kinesin-8 is a low-force motor protein with a weakly bound slip state. *Biophys. J.* 104:2456–2464.

44. Hancock, W. O. 2016. The kinesin-1 chemomechanical cycle: stepping toward a consensus. *Biophys. J.* 110:1216–1225.

45. Shimizu, T., K. Furusawa, …, R. D. Vale. 1991. Nucleotide specificity of the enzymatic and motile activities of dynein, kinesin, and heavy meromyosin. *J. Cell Biol.* 112:1189–1197.

46. Mickolajczyk, K. J., N. C. Deffenbaugh, …, W. O. Hancock. 2015. Kinetics of nucleotide-dependent structural transitions in the kinesin-1 hydrolysis cycle. *Proc. Natl. Acad. Sci. USA*. 112:E7186–E7193.